BASIC SCIENCE

Nanomedicine: Nanotechnology, Biology, and Medicine
13 (2017) 1289–1300

Original Article

nanomedjournal.com

An *in vitro* and *in vivo* study of peptide-functionalized nanoparticles for brain targeting: The importance of selective blood–brain barrier uptake

Gerard H. Bode[a], Gregory Coué[b], Christian Freese[c], Karin E. Pickl[d], Maria Sanchez-Purrà[e], Berta Albaiges[e], Salvador Borrós[e], Ewoud C. van Winden[f,1], Leto-Aikaterini Tziveleka[g], Zili Sideratou[g], Johan F.J. Engbersen[b], Smriti Singh[h], Krystyna Albrecht[i], Jürgen Groll[i], Martin Möller[h], Andy J.G. Pötgens[j], Christoph Schmitz[k], Eleonore Fröhlich[l], Christian Grandfils[m], Frank M. Sinner[d], C. James Kirkpatrick[c], Harry W.M. Steinbusch[a], Hans-Georg Frank[k], Ronald E. Unger[c], Pilar Martinez-Martinez[a,*]

[a]*Department of Neuroscience, School for Mental Health and Neuroscience, Faculty of Health, Medicine and Life Sciences, Maastricht University, Maastricht, The Netherlands*
[b]*Department of Biomedical Chemistry, MIRA Institute for Biomedical Technology & Technical Medicine, Faculty of Science and Technology, University of Twente, The Netherlands*
[c]*REPAIR-lab, Institute of Pathology, University Medical Center of the Johannes Gutenberg University Mainz and European Institute of Excellence on Tissue Engineering and Regenerative Medicine, Langenbeckstrasse 1, D-55101 Mainz, Germany*
[d]*HEALTH - Institute for Biomedicine and Health Sciences, Joanneum Research Forschungsgesellschaft m.b.H., Graz, Austria*
[e]*Grup d'Enginyeria de Materials (GEMAT), Institut Químic de Sarrià, Universitat Ramon Llull, Via Augusta 390, 08017 Barcelona, Spain*
[f]*Regulon AE, Koropi, Athens, Greece*
[g]*N. C.S.R. "Demokritos", Institute of Nanoscience and Nanotechnology, 15310 Aghia Paraskevi, Attiki, Greece*
[h]*DWI-Leibniz Institute for Interactive Materials, RWTH Aachen University, Forckenbeckstr. 50, 52074 Aachen, Germany*
[i]*Department of Functional Materials in Medicine and Dentistry, University of Würzburg, Pleicherwall 2, 97070 Würzburg, Germany*
[j]*AplaGen GmbH, Arnold-Sommerfeld-Ring 2, D-52499 Baesweiler, Germany*
[k]*Department of Neuroanatomy, Ludwig-Maximilians-University of Munich, Pettenkoferstrasse 11, 80336, Munich, Germany*
[l]*Center for Medical Research, Medical University of Graz, Graz, Austria*
[m]*Interfacultary Biomaterial Center (CEIB), University of Liege, Belgium*

Received 10 June 2016; accepted 17 November 2016

Abstract

Targeted delivery of drugs across endothelial barriers remains a formidable challenge, especially in the case of the brain, where the blood–brain barrier severely limits entry of drugs into the central nervous system. Nanoparticle-mediated transport of peptide/protein-based drugs across endothelial barriers shows great potential as a therapeutic strategy in a wide variety of diseases. Functionalizing nanoparticles with peptides allows for more efficient targeting to specific organs. We have evaluated the hemocompatibilty, cytotoxicity, endothelial uptake, efficacy of delivery and safety of liposome, hyperbranched polyester, poly(glycidol) and acrylamide-based nanoparticles functionalized with peptides targeting brain endothelial receptors, *in vitro* and *in vivo*. We used an ELISA-based method for the detection of nanoparticles in biological fluids, investigating the blood clearance rate and *in vivo* biodistribution of labeled nanoparticles in the brain after intravenous injection in Wistar rats. Herein, we provide a detailed report of *in vitro* and *in vivo* observations.

Key words: Nanoparticles; Peptides; Brain; Targeting

Grant support: EU FP6 NanoBioPharmaceutics Project no. 026723–2.
*Corresponding author at: Division Neuroscience, School for Mental Health and Neuroscience, Maastricht University, Universiteitssingel 50, 6229, ER, Maastricht, The Netherlands. Tel: +31 43 3881042; fax: +31 43 3884086.
E-mail address: p.martinez@maastrichtuniversity.nl (P. Martinez-Martinez).
[1] Current affiliation: Medochemie-Hellas, Greece.

http://dx.doi.org/10.1016/j.nano.2016.11.009
1549-9634/

Table 1
Overview of the peptides used to decorate nanoparticles.

Peptide name	Sequence	Modifications
5A	napvsipqKGGC	Biotin Carboxyfluorescein
15I	CGGKTFFYGGCRGKRNNFKTEEY	
NB03B	HKKWQFNSPFVPRADEPARKGKV HIPFPLDNITCRVPMAREPTVIHGKREVTLHLHPDH	TAMRA

Peptide 5A was used as a reporter peptide. Peptides 15I and NB03B were used as targeting peptides. Lower case amino acid letters denote D-amino acids and upper case L-amino acids.

Although considerable advances have been made in the last years towards understanding and treatment of central nervous system (CNS) disorders, it is still a major challenge to specifically target the brain using current pharmaceutics [1]. One of the obstacles a drug needs to overcome in order to reach the brain is the blood–brain barrier (BBB) [2]. The purpose of the BBB is both to ensure a constant environment within the CNS and to supply essential nutrients [3]. The BBB is formed by endothelial cell tight junctions in the microvessels of the brain. In contrast to peripheral capillaries, the BBB is more restrictive in the exchange of substances between blood and tissue parenchyma. However, contrary to what was first thought, the BBB is not impermeable and allows passage of proteins, such as antibodies and other pharmaceutical compounds, into the brain [4].

A possible way to improve delivery of drugs to the brain is the use of colloidal drug carriers such as nanoparticles (NPs), including liposomes, polymeric nanospheres and nanogels [3]. NPs can be loaded with peptides and proteins, facilitating their transfer across biological membranes. In addition, NPs protect their cargo against enzymatic degradation [5]. Thus, these complexes should be highly useful as targeted drug delivery systems.

Liposomes have attracted considerable attention as potential drug carriers that can be targeted to specific organs [6,7], including the brain [8,9]. Liposomes are small artificial vesicles of spherical shape which consist of an aqueous core entrapped by one or more bilayers composed of natural or synthetic, biocompatible and biodegradable lipids similar to biological membranes. The biophysical properties of liposomes such as size, surface charge, lipid composition and amount of cholesterol are variable and able to control distribution, tissue uptake and drug delivery [10].

Symmetric dendrimeric [11–13] and non-symmetric hyperbranched polymers [14,15], known as dendritic polymers, are nanometer-sized, highly branched macromolecules which consist of a central core, branching units and terminal functional groups. The existence of nanocavities, which can encapsulate various bioactive compounds, is their major structural feature. Furthermore, surface functionalization of dendritic polymers has been established as a successful approach for preparing a wide range of materials including drug delivery systems [16–18]. Another structural feature is the accumulation of a significant number of functional groups on their external surface. This has been proven to induce intense binding to multiple cell receptors due to the so-called multivalency effect [19,20].

Nanospheres have also been explored as drug carriers [21]. They are sub-micron-sized colloidal structures composed of synthetic and semi-synthetic polymers that vary in size from 1 to 1000 nm in which a drug can be dissolved or encapsulated. Compared with other colloidal carriers, polymeric nanospheres show higher stability when in contact with biological fluids. In addition, the use of biodegradable materials for nanoparticle preparation allows sustained drug release at the targeted site [22].

Nanogels are hydrophilic polymers cross-linked in porous networks capable of retaining water-soluble therapeutical peptides and proteins [23–25]. The typical size of nanogels is 10–400 nm. Therefore, they are large enough to avoid clearance from the circulation by glomerular filtration in the kidneys while small enough to limit clearance by the reticuloendothelial system [26]. Nanogels can be designed for stimulus-responsive degradation and drug release [27,28], and they have also been investigated as vehicles for drug delivery to the brain [29].

Both liposomes and nanospheres are usually rapidly cleared from the blood following intravenous administration. More than 90% of the NPs are removed from the blood stream within 5 min in mice [30,31]. Their surface modification with polysorbate 80, poly(ethylene glycol) (PEG) or poly(ethylene oxide) significantly alters the pharmacokinetics and the biological distribution of NPs [32–35].

Tissue specific targeting of NPs can be improved by coating them with peptides that bind to receptors on the target tissue [36]. Upon binding the receptor, the peptide-nanoparticle complex will be taken up by receptor-mediated endocytosis [37]. Receptors on brain endothelial cells, such as the low density lipoprotein receptor (LDLR), transferrin receptor and the insulin receptor can be used for this purpose [38,39].

Due to the potential of various NPs to be used as drug carriers, we have evaluated the efficacy of delivery and safety of liposome, functionalized hyperbranched polyester NPs, poly(-glycidol) based nanogels and two types of acrylamide-based NPs functionalized with peptides targeting brain endothelial receptors, *in vitro* and *in vivo*. Their hemocompatibility was assessed by *in vitro* assays, and their cytotoxicity and endothelial uptake were evaluated in various cell types. We investigated the blood clearance rate and *in vivo* biodistribution of labeled NPs in the brain after intravenous injection in Wistar rats.

Methods

Lipopolysaccharide/Endotoxin detection and cytotoxicity screening

Endotoxin content was determined by the PYROGENT Ultra Gel Clot LAL Assay (sensitivity 0.06 EU/ml; Lonza, Basel, Switzerland). The test was performed according to the information supplied by the manufacturer.

Table 2
Nomenclature of the nanoparticles used in the study and the peptides attached to the nanoparticles. All nanoparticles were coated with a reporter peptide. Additionally, some nanoparticles were coated with both a reporter and a targeting peptide.

Nanoparticle	Reporter peptide	Targeting peptide	Nomenclature nanoparticles (name nanoparticle + targeting peptide)
Liposomes	peptide 5A	none	Liposomes
	peptide 5A	peptide 15I	Liposomes-15I
	peptide 5A	NB03B	Liposomes-NB03B
BH40-polyester	peptide 5A	none	BH40-polyester
	peptide 5A	peptide 15I	BH40-polyester-15I
poly(amidoamine) (PAA)	peptide 5A	none	PAA
	peptide 5A	peptide 15I	PAA-15I
Acrylamide	peptide 5A	none	Acrylamide
	peptide 5A	peptide 15I	Acrylamide-15I
	peptide 5A	NB03B	Acrylamide-NB03B
poly(glycidol)	peptide 5A	none	poly(glycidol)
	peptide 5A	peptide 15I	poly(glycidol)-15I
	peptide 5A	NB03B	poly(glycidol)-NB03B

The human endothelial cell line EAhy926 (kind gift from Dr. C. J. Edgell) was used for evaluating the toxicity of the NPs. These cells were cultured at 37 °C in a humid 95% air/5% CO_2 atmosphere. Cells were seeded in DMEM, 10% FBS, 2 mM L-glutamine and 1% penicillin/streptomycin 24 h prior to the exposures. NP preparations were tested in concentrations up to 200 μg/ml of reporter peptide and three different assays were used to confirm the data. Viability was evaluated after 4 h and 24 h of exposure to NPs by formazan bioreduction using CellTiter 96 AQueous Non-Radioactive Cell Proliferation Assay (Promega, Mannheim, Germany) according to the manufacturer's instructions and a SPECTRA MAX plus 384 plate reader (Molecular Devices, Wals-Siezenheim, Austria).

In vitro hemocompatibility

The hemocompatibility of NPs was assessed by a panel of *in vitro* tests. NPs were incubated with whole blood for analysis of complement pathway activation, hemolysis and hemostasis activation as described [40].

Peptides

To evaluate the blood clearance rate and biodistribution of the NPs we attached the reporter peptide 5A to every NP. This peptide contained a carboxyfluorescein and a biotin group, allowing detection by ELISA. Additionally, we used brain targeting peptides 15I and NB03B. The amino acid sequence and modifications of these peptides are shown in Table 1.

Nanoparticles

In this study NPs of different chemical compositions were used: Liposomes, functionalized hyperbranched aliphatic polyester Boltorn H40 (BH40-polyester), Poly(amidoamine) (PAA), acrylamide and poly(glycidol) (Table 2). A brief description of the synthesis of these NPs is provided below and detailed synthetic routes can be found in the Supporting Information.

Liposomes

14.9 μmol of 1,2-Distearoyl-sn-glycero-3-phosphoethanolamine-N-[maleimide(polyethylene glycol)-2000 (DSPE-MAL) were reacted with 14.9 μmol of peptide 5A using a solution of 0.01 mM tris(2-carboxyethyl)phosphine (TCEP). Subsequently, liposomes were prepared by lipid film method. 316.8 μmol SPC and 148.5 μmol cholesterol were dissolved in the DSPE-MAL-peptide 5A mixture and heated to 60 °C under bath sonication. The batch was divided in 3 equal parts and DSPE-PEG was post-inserted by co-incubating for 1 h at 55 °C. Peptides NB03B and 15I were post-inserted by co-incubating the liposomes with an equimolar solution of DSPE-PEG-MAL and peptide for 1 h at 55 °C.

Hyperbranched polyester NPs

Hyperbranched aliphatic polyester Boltorn H40, (BH40, (M_n = 5100 g mol^{-1}, M_w/M_n = 1.8, hydroxyl number = 485 mg KOH/g) bearing 44 hydroxyl end groups was kindly donated by Perstorp AB, Sweden. BH40 with 32 carboxyl groups containing peptide 5A was prepared as described in the Supporting Information.

BH40-Polyester-15I was prepared by adding an equal volume of the targeting peptide 15I (3 mg/ml) to the preformed complex BH40-polyester/peptide 5A with a charge ratio *ca.* 4 and the solution was stirred and centrifuged. Finally, the supernatant solution was taken and uncomplexed peptides were removed by one-hour dialysis using a dialysis membrane with 3500 Da cut-off.

Poly(glycidol) based nanogels

Nanogels were synthesized *via* inverse mini-emulsion method [41,42]. For the preparation of the mini-emulsion, 37.5 mg of surfactant (3:1 weight ratio of Span 80 and Tween 80) were dissolved in 1.25 ml of n-hexane and was used as organic phase. The aqueous phase consisted of 50 mg (1.1×10^{-2} mM) of SH-PG and the respective peptides were dissolved in 125 μl of 0.04 M PBS buffer (pH 7.4). The organic and the aqueous phases were pre-emulsified by magnetic stirring for 10 minutes. After stirring, the system was ultrasonicated under ice cooling for 1 min. Crosslinking was initiated by subsequent addition of 30 μl of 0.1 M H_2O_2 followed by further sonication for 1 min. The reaction was allowed to proceed for 20 minutes at room temperature with constant stirring followed by quenching of the free thiol groups by 2-hydroxy ethyl acrylate at pH 7.4. Any further oxidation was stopped by addition of 1.5 ml of acidic water (pH 3). Separation of the nanogels was achieved by centrifugation at 10,000 rpm for 30 minutes followed by decantation of the supernatant. Nanogels present in the aqueous layer were carefully washed with hexane (2 × 1.5 ml) and THF (4 × 2.5 ml), dialysed and stored in DI water at 4 °C for further use.

Synthesis of Poly(amidoamine) NPs

A series of PAA polymers were synthesized *via* Michael polyaddition of the primary amine monomers, 4-amino-1-butanol (ABOL) and cPEG-NH_2, to the *N,N′*-cystaminebisacrylamide

Table 3
Summary of the cytotoxicity assay studies with the peptide-coated nanoparticles.

Nomenclature nanoparticle	Concentration (μg reporter peptide/ml)[a]	Cell viability[b]		Endotoxin (EU/mL)[c]	Hemcompatibility[d]			
		4 h	24 h		Hemolysis	Complement activation	Quick	APTT
Liposomes	200	105 ± 5	110 ± 4	<0.06	< 2%	380	100	100
Liposomes-15I	200	109 ± 9	105 ± 3	<0.06	< 2%	420	100	100
Liposomes-NB03B	200	107 ± 2	100 ± 2	<0.06	< 2%	700	100	100
BH40-polyester	200	101 ± 3	95 ± 4	<0.06	< 2%	150	100	30
BH40-polyester-15I	200	102 ± 2	99 ± 3	<0.06	< 2%	120	100	40
PAA	200	95 ± 5	96 ± 5	≥1	< 2%	136	98	100
PAA-15I	80	103 ± 2	85 ± 3	≥1	< 2%	189	97	100
Acrylamide	200	107 ± 4	105 ± 4	<0.06	< 2%	100	100	100
Acrylamide-15I	200	100 ± 5	96 ± 6	<0.06	< 2%	115	95	99
Acrylamide-NB03B	200	98 ± 3	104 ± 4	<0.06	< 2%	110	98	97
poly(glycidol)	250	98 ± 4	100 ± 1	<0.06	< 2%	105	99	96
poly(glycidol)-15I	250	90 ± 7	98 ± 6	<0.06	< 2%	110	95	98
poly(glycidol)-NB03B	250	98 ± 3	95 ± 1	<0.06	< 2%	107	98	99

[a] The concentrations shown are determined by the amount of reporter peptide coated on the nanoparticles. [b]The viability was determined by MTT reduction of EAhy926 cells incubated with nanoparticles at the concentration shown in column 2. [c]Endotoxin levels were quantified using a commercial assay. Values of <0.06 are below the detection threshold. [d]Hemocompatibility data include: hemolysis, complement activation, and hemostasis activation (Quick and TCA) after a 15 min incubation of the NPs at 37 °C in whole blood. Hemolysis percent represent free plasma hemoglobin released as a result of contact with the test material divided by the total blood hemoglobin multiplied by 100. Complement activation is expressed as a % of C3a concentration, adopting normal blood incubated in the same conditions as 100%. Ctrl + : blood incubated with Zymosan. Quick and TCA hemostasis assays are reported in % of the clotting ability of the sample compared to the clotting ability of a standard human plasma normalized to 100.

(CBA) using equimolar monomeric amine/acrylamide ratios. For the synthesis of p(CBA-ABOL/cPEG-NH_2), a co-polymer aiming for 10% PEG side chains, CBA (2.63 g, 10 mmol), ABOL (0.89 g, 9.8 mmol) and cPEG-NH_2 (0.67 g, 0.2 mmol) were dissolved in 5 ml MeOH/DI water (4/1 v/v) mixture.

Peptide 5A was dissolved in a PBS/EtOH solution and incubated with the cPEG-p(CBA-ABOL) polymers at a 12:1 polymer:peptide ratio.

A similar procedure was carried out for the synthesis of p(BAP-ABOL/cPEG-NH_2). The terminal carboxylic acid group present in the side chains of the polymer p(BAP-ABOL/cPEG-NH_2) (200 mg) was activated using EDC (66 mg) and sulfo-NHS (67 mg) in HEPES buffer (10 mM, pH 8). Then, the targeting peptide 15I (15 mg) dissolved in a mixture of HEPES buffer (10 mM, pH 8) and EtOH (3/2 v/v) was added to the mixture.

To prepare the nanosystems with targeting peptide 15I, a similar formulation procedure as previously described was followed, except that 100 μl out of the 800 μl of polymer used were substituted with targeting peptide-grafted polymer p(BAP-ABOL/15I–g-cPEG-NH_2).

Synthesis of Acrylamide NPs

Acrylamide NPs were synthesized by the free-radical polymerization method in a microemulsion system as described [43], where the monomers used were *N*-isopropylacrylamide, *N,N′*-dimethylacrylamide and acrylic acid, the cross-linker was methylenebisacrylamide, the surfactant, sodium dodecyl sulfate, and the initiator, ammonium persulphate.

In vitro uptake of NPs

The human cerebral microvascular endothelial cell line, hCMEC/D3, was provided by the group of Pierre-Olivier Couraud (Department of Cell Biology, Institut Cochin, Paris, France) and was first characterized by Weksler et al. [44]. The cells were cultured on fibronectin-coated culture flasks in endothelial cell basal medium (ECBM; Customer Formulation) supplemented with 15% fetal bovine serum, 2.5 ng/ml basal fibroblast growth factor and 10 μg/ml sodium heparin (both Sigma-Aldrich, St. Luis, USA), and 10,000 units/ml penicillin/10,000 μg/ml streptomycin (both Gibco, Carlsbad, USA).

Cells were seeded onto fibronectin-coated LabTek chamber slides (Nunc, Roskilde, Denmark) in ECBM culture medium (surface 0.7cm^2/well). After 48 h cells were incubated with 200 μl of various nanoparticle-ECBM suspensions. After the incubation period, cells were washed twice with HEPES buffer including 0.2% BSA and then fixed with 3.7% paraformaldehyde at room temperature for 20 min. Afterwards, cells were washed and incubated with mouse anti-human CD31 antibody (DakoCytomation, Glostrup, Denmark) and the corresponding secondary antibody (goat anti-mouse Alexa Fluor 546; Molecular Probes, Carlsbad, USA) at RT for 1 hour each. The nuclei were stained with Hoechst 33,342 (Sigma-Aldrich). The LabTeks were embedded with GelMount (Biomeda, Natutec, Germany) and analyzed by fluorescence microscopy (Olympus IX71 with Delta Vision system, Applied Precision, USA).

Animals and tissue preparation

2 month old male Wistar rats were obtained from Harlan (Indianapolis, IN). The animals were housed three per cage with *ad libitum* food and water and a 12:12 hour light:dark cycle. All animal experiments complied with Dutch law and were approved by the ethical committee of Maastricht University. All animals received humane care in accordance with institutional guidelines.

Three animals per time point were used for each NP. After intravenous injection of NP formulations containing 0.5 mg

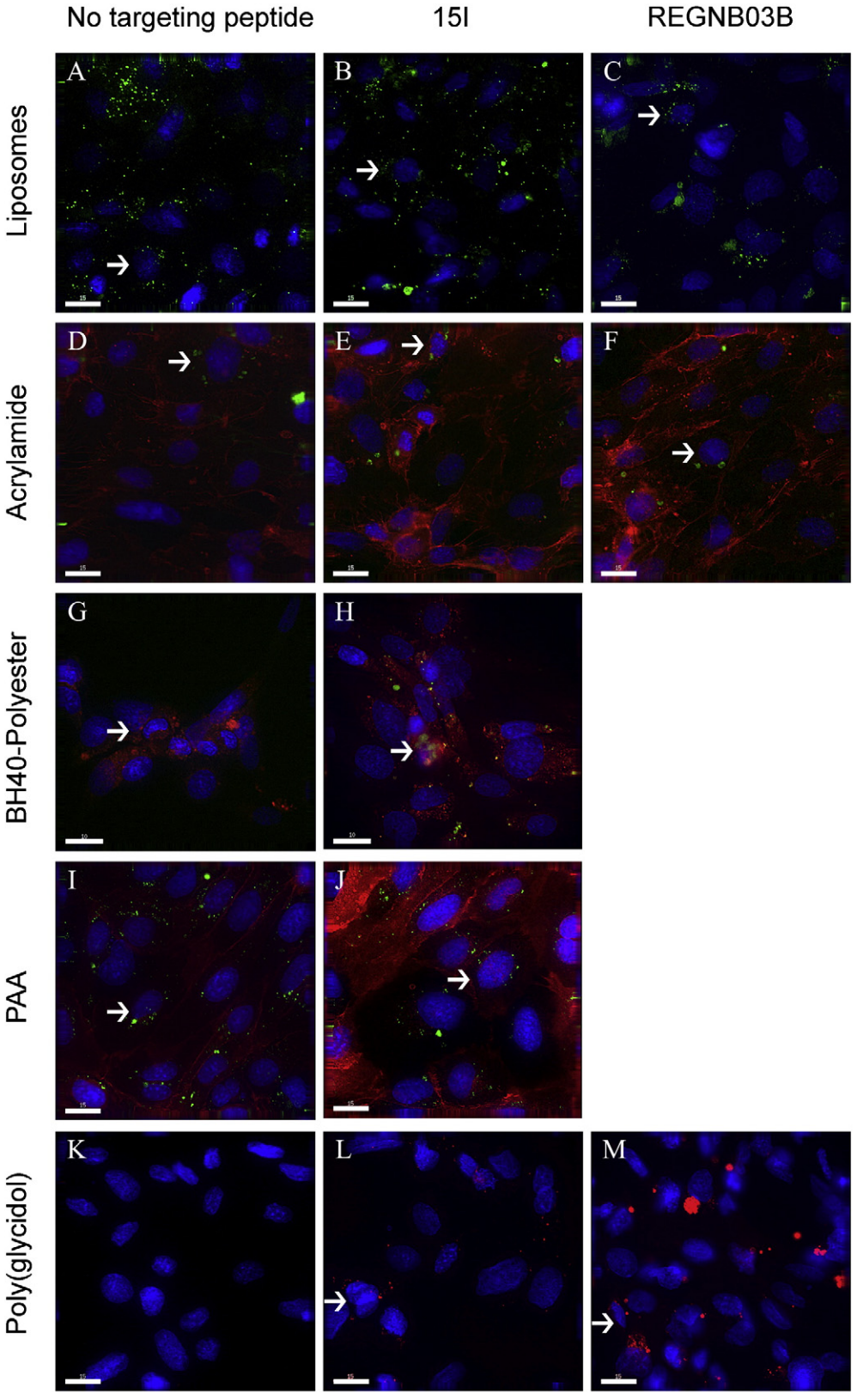

Figure 1. Evaluation of nanoparticle uptake by brain endothelial cells (hCMEC/D3). hCMEC/D3 cells were incubated with different nanoparticles containing a fluorescently labeled reporter peptide, and coated with or without targeting peptides 15I and NB03B for 24 h. Representative fluorescent microscopy pictures showing uptake of liposomes **(A-C)**, acrylamide **(D-F)**, polyester (**G** and **H**), PAA-based (**I** and **J**) nanoparticles and poly(glycidol) nanogels **(K-M)**. Cell membranes were stained with anti-CD31 antibody (D-F and H-I, shown in red). The BH40-polyester nanoparticles were directly labeled with rhodamine. Cell nuclei were stained with Hoechst dye (blue). Arrows indicate cells containing nanoparticles.

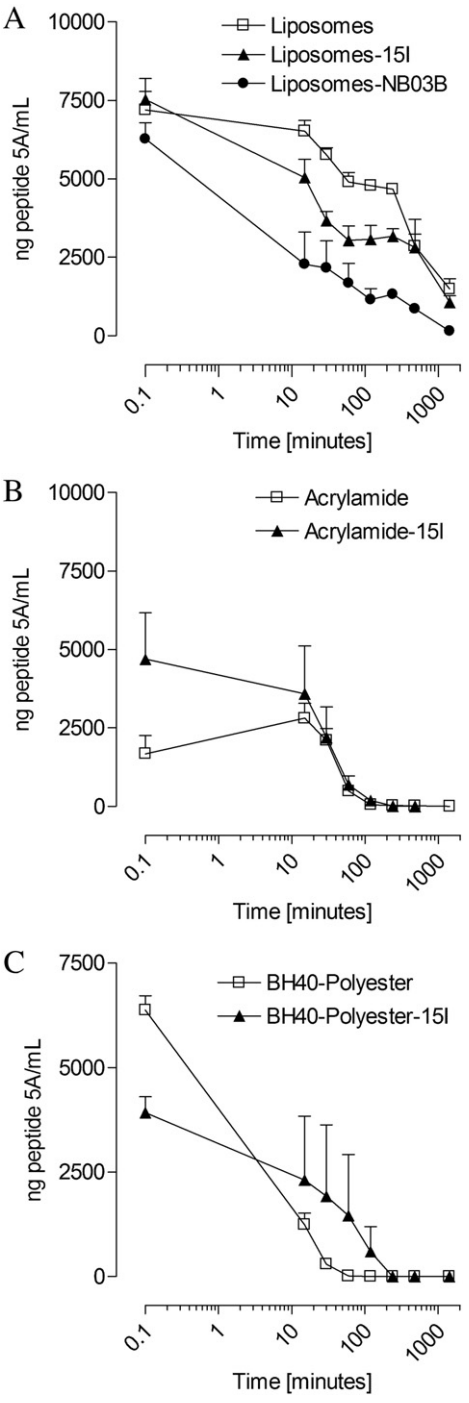

Figure 2. Blood plasma concentration of peptide 5A containing nanoparticles after intravenous injection in rats. Blood was taken immediately and at 15, 30, 60 minutes and at 2, 4, 8 and 24 hours after injection from the tail vein. Plasma was prepared and peptide 5A concentration was measured by ELISA. All nanoparticles contained the reporter peptide 5A, and were coated with or without targeting peptides 15I and NB03B. Liposomes were detected in plasma up to 24 hours after injection **(A)** while the other nanoparticles were not detectable in plasma after 4 hours (**B** and **C**). Data are shown on a logarithmic time scale as the mean ± S.E.M. plasma concentration of peptide 5A in 3 animals per nanoparticle.

peptide 5A /kg, the animals were anesthetized and either decapitated (unperfused) or transcardially perfused with Tyrode's buffer for 10 minutes to remove residual blood. Subsequently, the brain and liver were dissected and either flash frozen in liquid nitrogen for analysis by ELISA or frozen on a metal platform partially submerged in liquid nitrogen for analysis by immunohistochemistry. CSF was collected before sacrificing the animals. All samples were stored at −80 °C until further analysis.

ELISA for the detection of peptide 5A

Streptavidin coated ELISA 96-well-microplates (Steffens Biotechnische Analysen, Ebringen, Germany) were used for the detection of 5A in plasma and tissue samples as described [43]. Briefly, the carboxyfluorescein group present on the reporter peptide was detected by incubating with monoclonal mouse-anti-fluorescein peroxidase-conjugated IgG (Dianova, Hamburg, Germany) diluted 1:100,000 in PBS with 0.1% BSA for one hour. Soluble high sensitivity TMB (SDT, Baesweiler, Germany) was used as a chromogenic substrate to visualize bound antibody.

Peptide 5A detection in blood plasma, brain, liver and cerebrospinal fluid after intravenous injection

Detection of peptide 5A in blood plasma was performed as described [43]. The brain, liver and cerebrospinal fluid (CSF) of 3 animals per time point were analyzed for peptide 5A content by ELISA. Tissue samples were homogenized in lysis buffer (137 mM NaCl, 20 mM Tris, 10% glycerol, 1% IGEPAL *CA*-630 (Sigma), pH 7.4) at a weight to volume ratio of 1:4 in a tube containing Lysing Matrix D (MP Biomedicals, Santa Ana, *CA*). Samples were cooled on ice before and between four rounds of homogenization for 30 seconds in a mini-beadbeater (Biospec, Bartlesville, OK).

Detection of injected nanoparticles in rat tissue by immunohistochemistry

10 μm thick cryosections were fixed with Somogyi fixative containing glutaraldehyde, blocked with 0.3% H_2O_2 and probed with monoclonal mouse-anti-fluorescein peroxidase-conjugated IgG (Dianova, Hamburg, Germany). Peroxidase activity was visualized with DAB substrate. For immunofluorescence microscopy, the tyramide signal amplification system (Perkin Elmer) was used in conjunction with Alexa fluor 488 labeled streptavidin. As a negative control, the primary antibody was omitted. Brightfield photomicrographs were acquired on an AX70 microscopy workstation (Olympus, Shinjuku, Tokyo, Japan) and fluorescence photomicrographs were acquired on an Olympus BX81 with a disk scanning unit.

Results

In vitro cytotoxicity and hemocompatibility of NPs

The NPs listed in Table 2 were tested for the presence of endotoxin contamination and potential cytotoxic effects using EAhy926 endothelial cells. Viability of the cells was tested after 4 hours and 24 hours of incubation with the NPs. No decrease in viability was observed for any of the NPs, as evaluated by formazan bioreduction (see Table 3). In addition, most of the samples showed less than 0.6 EU of endotoxin measured by LAL

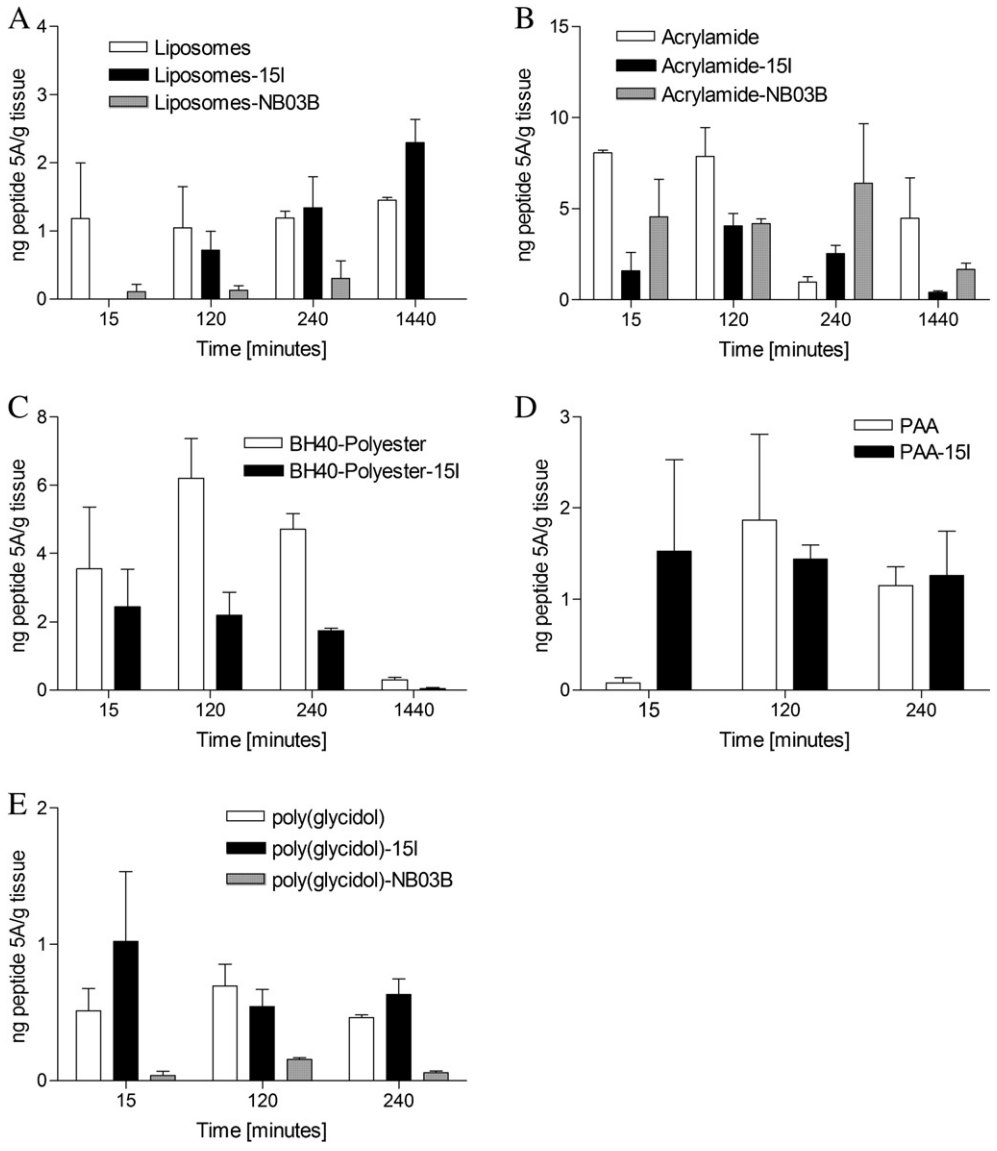

Figure 3. Concentration of peptide 5A in brain homogenate after intravenous injection of nanoparticles. Animals were sacrificed at different time points after injection and the concentration of peptide 5A in brain homogenate was measured by ELISA. All nanoparticles contained the reporter peptide 5A, and were either coated with targeting peptides 15I and NB03B, or not. Data are shown as the mean ± S.E.M. peptide 5A concentration of 3 animals.

assay. The PAA NPs and in some cases poly(glycidol) nanogels tested at more than 1 EU (see Table 3). In the case of nanogels, these contaminations resulted from contaminated water during nanogel purification and these samples were not used for *in vivo* studies. Cell morphology was not affected by the NPs (data not shown).

Additionally, the hemocompatibility of these NPs was evaluated *in vitro* using human blood (Table 3). Several toxicological reactions potentially occur when NPs are diluted in the blood stream, in particular: Embolisation, hemolysis, cellular activation, but also biological cascades such as coagulation, complement activation, kinin/kininogen, fibrinolysis. Moreover, if one wants to target nanoparticles, the first barrier that the material will encounter is the blood itself and the Reticulo-Endothelial System (RES). All of the NPs tested showed good hemocompatibility without any severe adverse reactions.

Uptake of NPs in vitro by human brain endothelial cells

The uptake of NPs with and without targeting peptides 15I and NB03B in the human cerebral microvascular endothelial cell line hCMEC/D3 was studied. Four different NP compositions were used, containing the reporter peptide 5A (Figure 1 *A-J*) or Rhodamine (Figure 1 *K-L*) as a label. Uptake of NPs was observed in all conditions studied for liposomes (A-C), acrylamide (D-F), BH40-polyester (G-H) and PAA (I-J) NPs. In contrast, uptake of poly(glycidol) nanogels was seen only when the nanogels contained a targeting peptide (K-M).

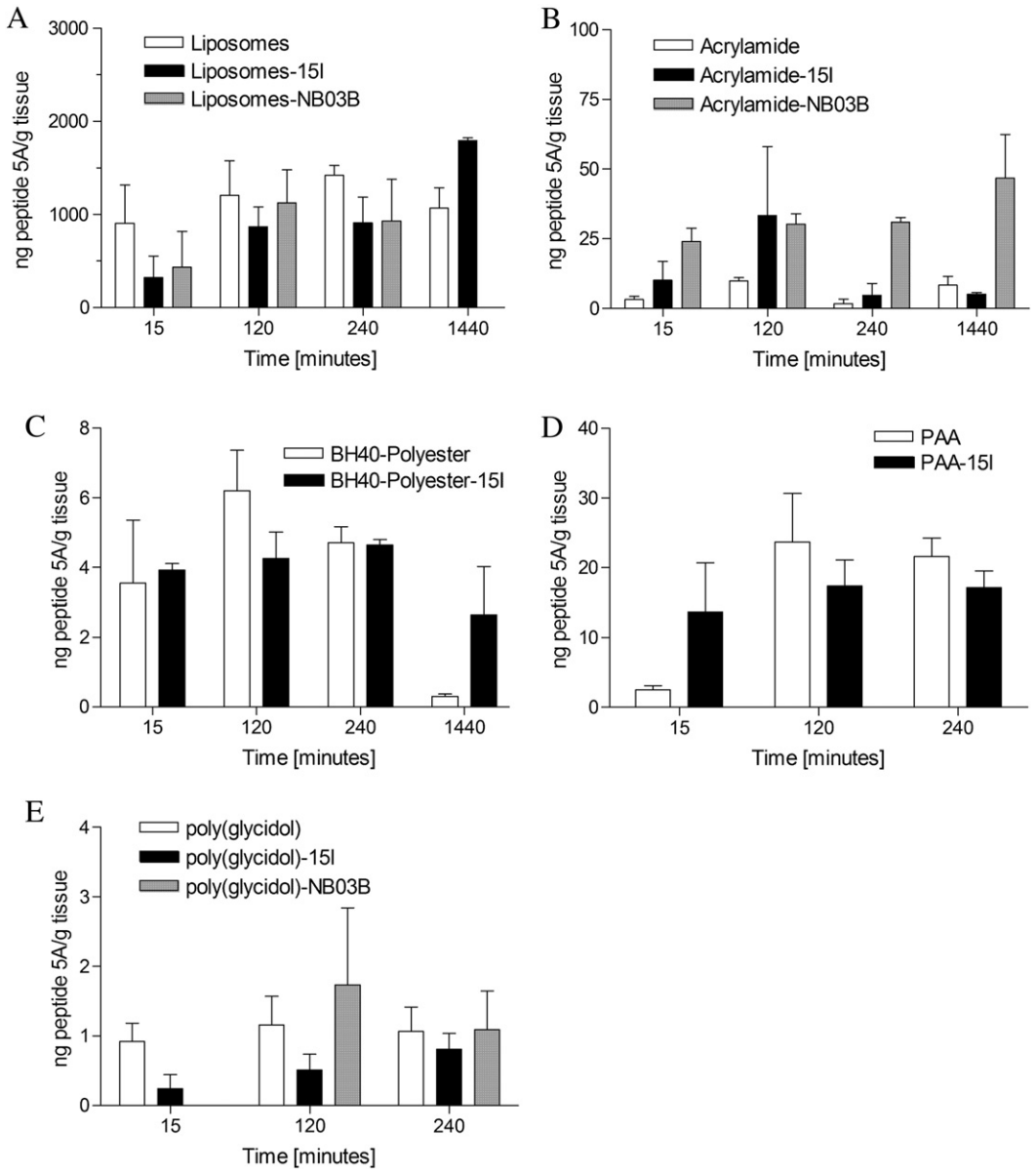

Figure 4. Concentration of peptide 5A in liver homogenate after intravenous injection of nanoparticles. Animals were sacrificed at different time points after injection and the concentration of peptide 5A in liver homogenate was measured by ELISA. All nanoparticles contained the reporter peptide 5A, and were either coated with targeting peptides 15I and NB03B or not. The combination of Liposomes with NB03B was not measured at 1440 minutes (A). Data are shown as the mean ± S.E.M. peptide 5A concentration of 3 animals.

Plasma concentrations of intravenously injected NPs

The aim of the next experiment was to determine the time that the NPs remained in circulation and whether this was affected by the presence of a targeting peptide. For this purpose we intravenously injected NPs (Table 2) in Wistar rats, collected repeated blood plasma samples and measured peptide 5A concentration by ELISA. For the majority of the NPs injected, we were able to detect the attached peptide 5A in plasma (Figure 2, *A-C* and Figure S1). In Figure 2, *A*, we show that the peptide 5A attached to liposomes was detected up to 24 hours after injection. In contrast, peptide 5A attached to acrylamide, BH40-Polyester, PAA NPs and poly(glycidol) nanogels was only detected up to 2 hours. When 15I or NB03B targeting peptides were anchored to liposomes, a reduction of peptide 5A plasma concentration by 36 and 64%, respectively, 30 minutes after injection was observed (Figure 2, *A*). The 64% reduction in plasma concentration observed with NB03B liposomes suggests faster elimination from the circulation in the presence of this peptide, possibly due to increased uptake.

In contrast, no clear effect of the targeting peptides on peptide 5A concentration was observed when acrylamide (Figure 2, *B*) hyperbranched polyester (Figure 2, *C*), and poly(amidoamine) (Figure S1, *A*) NPs as well as poly(glycidol) nanogels (Figure S1, *B*) were used.

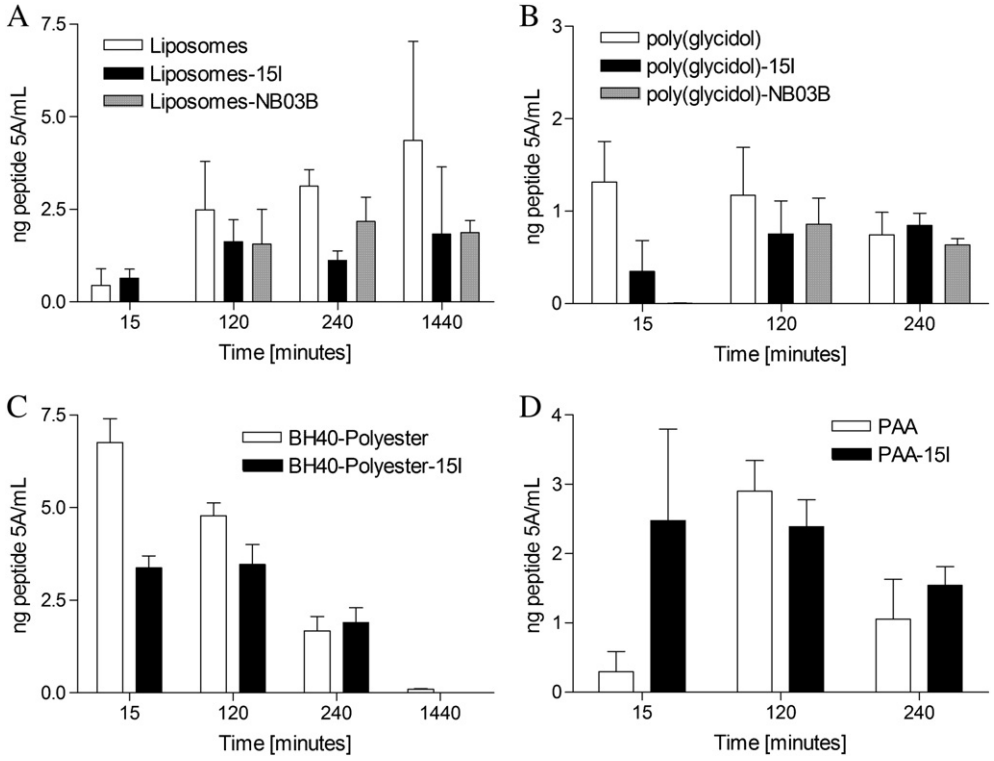

Figure 5. Concentration of peptide 5A in CSF after intravenous injection of nanoparticles. Animals were sacrificed at different time points after injection and the concentration of peptide 5A in CSF was measured by ELISA. All nanoparticles contained the reporter peptide 5A, and were coated with or without targeting peptides 15I and NB03B. The presence of targeting peptides on the nanoparticles did not result in increased peptide 5A concentration in the CSF **(A-C)**. A higher concentration of peptide 5A was observed 15 minutes after injection PAA-15I nanoparticles compared to PAA nanoparticles without 15I targeting peptide **(D)**. Data are shown as the mean ± S.E.M. peptide 5A concentration of 3 animals.

Detection of NPs in the brain, liver and CSF

To determine whether the NP compositions listed in Table 2 reached the brain, ELISA and immunohistochemistry methods were used to detect peptide 5A in brain tissue from intravenously injected animals. To avoid contamination of brain tissue samples with blood from the brain vasculature, the animals were transcardially perfused before removal of the brain at the time of sacrifice. Peptide 5A was detected in brain homogenates by ELISA (Figure 3), although the amount of peptide was below 10 ng per gram of tissue for all NP-peptide combinations. Interestingly, when the targeting peptide 15I or NB03B were anchored to liposomes, the concentration of peptide 5A in the brain increased over time (Figure 3, *A*). Addition of targeting peptides to acrylamide NPs did not result in a difference in peptide 5A concentrations in the brain compared to non-targeted NPs (Figure 3, *B*). For BH40-Polyester NPs, lower peptide 5A concentrations with 15I were observed at 2 hours ($p < 0.05$), 4 hours ($p < 0.01$) and 24 hours ($p < 0.05$). The same pattern was observed with poly(glycidol) nanogels containing NB03B targeting peptide (Figure 3, *E*), suggesting that the co-presence of the targeting and reporter peptides result in a reduced brain uptake. No difference in peptide 5A concentration was observed between PAA NPs with and without 15I targeting peptide (Figure 5, *D*).

Because of the role of the liver in the clearance of NPs, peptide 5A concentration was also determined in liver homogenates of the same animals (Figure 4). The highest concentrations of peptide 5A were detected in animals injected with liposomes (Figure 4, *A*) compared to the other NP compositions (Figure 4, *B-E*) where the concentrations detected were significantly lower. Compared to non-targeted liposomes, we observed an increase over time of 15I–liposomes, with the highest concentration after 24 hours ($p < 0.05$). The addition of NB03B targeting peptide to acrylamide NPs resulted in higher uptake of these NPs by the liver at 15 minutes ($p < 0.01$), 2 hours ($p < 0.05$) and 4 hours ($p < 0.01$) (Figure 4, *B*). No statistically significant differences in liver uptake were observed between non-targeted and targeted BH40-Polyester and PAA NPs and also poly(glycidol) nanogels. Furthermore, BH40-Polyster NP and poly(glycidol) nanogel accumulation in the liver was low, as expected, due to their hydrophilic nature.

In parallel to the brain homogenate measurements, we studied whether NPs were present in CSF collected from the same animals described above. Peptide 5A was detected in the CSF of liposome-injected animals up to 24 hours after injection (Figure 5, *A*). Moreover, with the concentration of peptide 5A in CSF (Figure 5, *A-D*) tended to show the same pattern as in brain homogenate (Figure 3).

Immunohistochemical analysis of unperfused brain and liver tissue obtained from rats injected with peptide 5A/NB03B loaded liposomes revealed the presence of peptide 5A in the

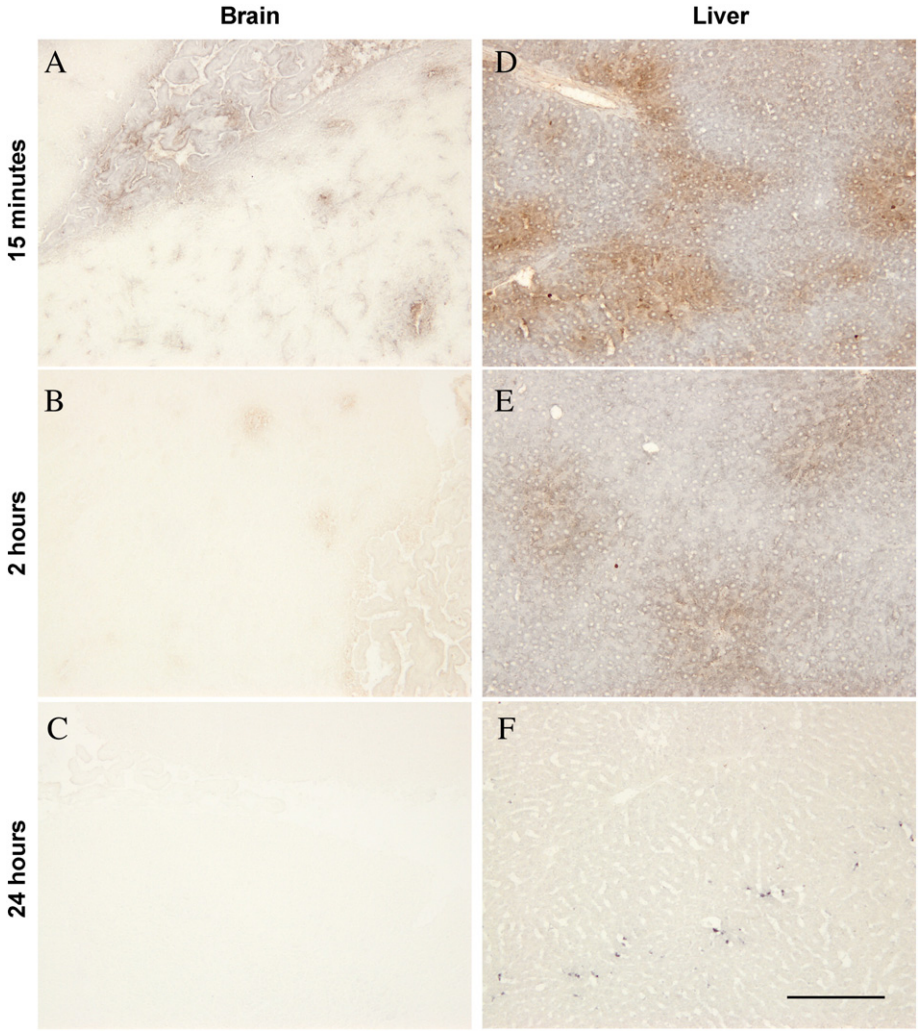

Figure 6. Immunohistochemical detection of peptide 5A in brain (A-C) and liver (D-F) tissue sections injected with liposomes containing peptides 5A and NB03B. Peptide 5A was detected with a monoclonal antibody against FITC in brain tissue sections of animals sacrificed without transcardial perfusion 15 minutes **(A)**, 2 hours **(B)** and 24 hours **(C)** after injection. 3 animals per time point were analyzed and representative images are shown. Brain and liver photomicrographs from the same animal are shown on each row. Scale bar is 200 μm.

choroid plexus and surrounding blood vessel-like structures (Figures 6 and 7). The strongest staining in the brain was observed 15 minutes after injection (Figure 6, *A*), compared to weaker staining 2 hours after injection (Figure 6, *B*) and almost undetectable levels 24 hours after injection (Figure 6, *C*). Liver tissue from the same animals showed a similar pattern over time (Figure 6, *D-F*). In contrast, peptide 5A was undetectable by immunohistochemistry in the brains of animals that were transcardially perfused after injection with peptide 5A/NB03B loaded liposomes (data not shown).

Discussion

The aim of this study was the development of NPs functionalized with targeting peptides for specific brain delivery. We report the synthesis of different types of NPs (liposomes, hyperbranched polyester, poly(glycidol) and acrylamide based) conjugated to targeting peptides. Important NP design considerations were their ability to carry peptide/protein cargo and their biodegradable nature. The NPs were labeled with a reporter peptide containing biotin and fluorescein (peptide 5A), and with different peptides containing targeting properties based on the angiopep sequence (peptide 15I) and a novel peptide based on a Semliki forest virus (SFV) protein (NB03B). Angiopep peptides are derived from the Kunitz domain of aprotinin and have been proposed as a suitable brain delivery system by utilizing receptor mediated transcytosis *via* the low-density lipoprotein receptor-related protein at the BBB [45]. The SFV is a neuroinvasive virus that is thought to cross the BBB [46]. We used a peptide based on a SFV protein with the potential to bind and cross brain endothelial cells. Since the safety of nanomaterials is an important consideration [47,48], initially all NPs were screened for *in vitro* cytotoxicity and hemocompatibility, and subsequently only the NPs that did not show significant adverse effects were used for *in vivo* studies. In line with the *in vitro* toxicity and

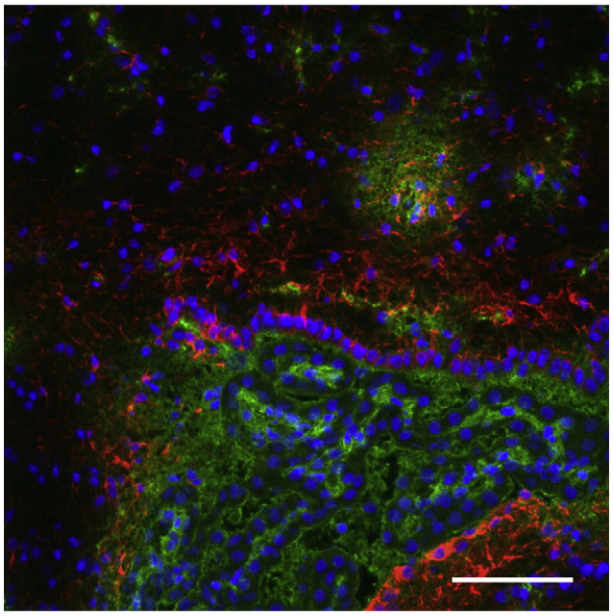

Figure 7. Fluorescence immunohistochemistry of FITC labeled reporter peptide 5A in brain tissue. A 10 μm brain section of an unperfused 2 month old Wistar rats 15 minutes after injection with peptide 5A liposomes containing NB03B targeting peptide was stained for FITC and GFAP. Green channel: FITC labeled peptide 5A; Red channel: Astrocyte marker GFAP; Blue channel: Nucleus (Hoechst). Scale bar is 50 μm.

hemocompatibility experiments, none of the injected NP formulations showed any signs of acute toxicity or other adverse effects *in vivo*.

Additionally we evaluated the selective uptake of NP compositions by brain endothelial cells (ECs). The representative images in Figure 1 indicate that the NP can be internalized by brain ECs and that as a consequence a transcytosis of the NPs across the cells may be possible. However, the fact that NPs without targeting peptides showed uptake indicates that they might not be internalized by a receptor-mediated pathway, except for the poly(glycidol) based nanogels, which show *in vitro* uptake only when the nanogels contained either the targeting peptide. It is important to mention that we determined the total amount of peptide attached to the mix of NPs for each formulation, but, the distribution, number of peptides and the accessibility of the peptide per single NP was not determined. Since it is known that physico-chemical properties of NPs are also responsible for cell-nanoparticle interactions, the uptake of those in brain endothelial cells *in vitro* may be explained. As shown by Kasper et al. and Freese et al. [49,50], the uptake of silica and polymer-modified gold NPs of different sizes was mediated by a clathrin- and caveolin-1 independent pathway as described by Glebov et al. [51] which demonstrates that binding to a specific receptor is not essential for nanoparticle uptake. We have to take into account that the semi-quantitative analysis of the *in vitro* uptake images might not have been sensitive enough to observe small differences which could account for the detected accumulation in the brain.

The effect of targeting peptides on the blood clearance rate and biodistribution of the NPs was studied after intravenous injection in Wistar rats. After analyzing brain homogenates, no preferential uptake of the NPs in brain tissue could be detected. Thus the *in vivo* experiments are in accordance with the results shown in the *in vitro* studies. In line with these results, a recent study showed no increase in brain uptake of the enzyme arylsulfatase A when conjugated to angiopep [52]. In contrast, it has been shown that conjugating angiopep-2 to neurotensin results in a ten-fold increase in brain uptake [53], and it has been reported that angiopep increases uptake of lipid based NPs 2.4-fold *in vitro* [54].

A fraction of the NPs did reach the brain as confirmed by the ELISA results showing low accumulation of NPs in brain homogenates and CSF. In addition, we detected the fluorescent label on liposomes in the brain of unperfused animals by immunofluorescence microscopy. In contrast, perfusing the brain after injection of liposomes resulted in markedly decreased immunofluorescent signal, limited to the choroid plexus.

Liver homogenate concentrations of acrylamide, BH40-polyester, PAA and poly(glycidol) were similar to those found in brain homogenates while a larger fraction of the injected dose of liposomes was found in the liver. This indicates that the liver only plays a significant role in NP clearance for liposomes.

The low amounts of NPs detected in the brain could be explained by the following factors: i) the combinations of NPs and targeting peptides did not show sufficient specificity for brain endothelial cells as shown in our *in vitro* experiments; ii) the low stability of the nanoparticle-peptide complex *in vivo e.g.* due to enzymatic degradation of the targeting peptide and/or reporter label [55].

Interestingly, the anchoring of targeting peptides to liposomes resulted in altered blood plasma levels, with increased clearance from the circulation.

In this study, various formulations with different physicochemical properties were evaluated. The obtained results further strengthen the concept that structural and physicochemical characteristics of NPs define their cellular uptake and biodistribution. Therefore, the successful uptake cannot be attributed only to the presence of the targeting ligand but also to the nature of the NPs. It is also important to note that localization and accessibility of the targeting peptides in NPs might also play a role in the efficacy of the targeting. In conclusion, in order to improve brain targeting of NPs, it is essential that the combination of physical characteristics of the NPs and the targeting peptides confer high specificity for brain endothelial cells *versus* other endothelial cells in different organs.

Appendix A. Supplementary data

Supplementary data to this article can be found online at http://dx.doi.org/10.1016/j.nano.2016.11.009.

References

1. Yi X, et al. Agile delivery of protein therapeutics to CNS. *J Control Release* 2014;**190**:637-63.
2. Georgieva JV, Hoekstra D, Zuhorn IS. Smuggling drugs into the brain: an overview of ligands targeting Transcytosis for drug delivery across the blood–brain barrier. *Pharmaceutics* 2014;**6**(4):557-83.

3. Brasnjevic I, et al. Delivery of peptide and protein drugs over the blood–brain barrier. *Prog Neurobiol* 2009;**87**(4):212-51.
4. Martinez-Martinez P, et al. Autoantibodies to neurotransmitter receptors and ion channels: from neuromuscular to neuropsychiatric disorders. *Front Genet* 2013;**4**:181.
5. Petros RA, DeSimone JM. Strategies in the design of nanoparticles for therapeutic applications. *Nat Rev Drug Discov* 2010;**9**(8):615-27.
6. Eloy JO, et al. Liposomes as carriers of hydrophilic small molecule drugs: strategies to enhance encapsulation and delivery. *Colloids Surf B Biointerfaces* 2014;**123**:345-63.
7. Deshpande PP, Biswas S, Torchilin VP. Current trends in the use of liposomes for tumor targeting. *Nanomedicine (Lond)* 2013;**8**(9):1509-28.
8. Rotman M, et al. Enhanced glutathione PEGylated liposomal brain delivery of an anti-amyloid single domain antibody fragment in a mouse model for Alzheimer's disease. *J Control Release* 2015;**203**:40-50.
9. Kuo YC, Lin CC. *Rescuing Apoptotic Neurons in Alzheimer's Disease Using Wheat Germ Agglutinin-Conjugated and Cardiolipin-Conjugated Liposomes with Encapsulated Nerve Growth Factor and Curcumin*; 2015 (1178–2013 (Electronic)).
10. van der Meel R, et al. Extracellular vesicles as drug delivery systems: lessons from the liposome field. *J Control Release* 2014;**195**:72-85.
11. Fréchet JMJ, Tomalia DA. *Dendrimers and other dendritic polymers*. Polymer Science; 2001.
12. Newkome G, Moorefield C, Vögtle F. *Dendritic Molecules: Concepts, Synthesis, Perspectives*; 1996.
13. Bosman AW, Janssen HM, Meijer EW. About dendrimers: structure, physical properties, and applications. *Chem Rev* 1999;**99**(7):1665-88.
14. Huang Y, et al. Synthesis and therapeutic applications of biocompatible or biodegradable hyperbranched polymers. *Polymer Chemistry* 2015;**6**:2794-812.
15. Calderon M, et al. Dendritic polyglycerols for biomedical applications. *Adv Mater* 2010;**22**(2):190-218.
16. Paleos CM, et al. Drug delivery using multifunctional dendrimers and hyperbranched polymers. *Expert Opin Drug Deliv* 2010;**7**(12):1387-98.
17. Gillies ER, Frechet JM. Dendrimers and dendritic polymers in drug delivery. *Drug Discov Today* 2005;**10**(1):35-43.
18. Khandare J, et al. Multifunctional dendritic polymers in nanomedicine: opportunities and challenges. *Chem Soc Rev* 2012;**41**(7):2824-48.
19. Mammen M, Choi S-K, Whitesides GM. Polyvalent interactions in biological systems: implications for design and use of multivalent ligands and inhibitors. *Angew Chem Int Ed* 1998;**37**(20):2754-94.
20. Fasting C, et al. Multivalency as a chemical organization and action principle. *Angew Chem Int Ed* 2012;**51**(42):10472-98.
21. Herran E, et al. Increased antiparkinson efficacy of the combined administration of VEGF- and GDNF-loaded nanospheres in a partial lesion model of Parkinson's disease. *Int J Nanomedicine* 2014;**9**:2677-87.
22. Vinogradov SV, Bronich TK, Kabanov AV. Nanosized cationic hydrogels for drug delivery: preparation, properties and interactions with cells. *Adv Drug Deliv Rev* 2002;**54**(1):135-47.
23. Vermonden T, Censi R, Hennink WE. Hydrogels for protein delivery. *Chem Rev* 2012;**112**(5):2853-88.
24. Chacko RT, et al. Polymer nanogels: a versatile nanoscopic drug delivery platform. *Adv Drug Deliv Rev* 2012;**64**(9):836-51.
25. Albrecht K, Moeller M, Groll J. In: Pich A, Richtering W, editors. *Nano- and Microgels through Addition Reactions of Functional Oligomers and Polymers, in Chemical Design of Responsive Microgels*. Berlin Heidelberg: Springer; 2011. p. 65-93.
26. Letchford K, Burt H. A review of the formation and classification of amphiphilic block copolymer nanoparticulate structures: micelles, nanospheres, nanocapsules and polymersomes. *Eur J Pharm Biopharm* 2007;**65**(3):259-69.
27. Zha L, Banik B, Alexis F. Stimulus responsive nanogels for drug delivery. *Soft Matter* 2011;**7**(13):5908-16.
28. Singh S, et al. Embedding of active proteins and living cells in redox-sensitive hydrogels and nanogels through enzymatic cross-linking. *Angew Chem Int Ed Engl* 2013;**52**(10):3000-3.
29. Azadi A, Hamidi M, Rouini MR. Methotrexate-loaded chitosan nanogels as 'Trojan horses' for drug delivery to brain: preparation and in vitro/in vivo characterization. *Int J Biol Macromol* 2013;**62**:523-30.
30. Pardridge WM. Recent developments in peptide drug delivery to the brain. *Pharmacol Toxicol* 1992;**71**(1):3-10.
31. Olivier JC, et al. Indirect evidence that drug brain targeting using polysorbate 80-coated polybutylcyanoacrylate nanoparticles is related to toxicity. *Pharm Res* 1999;**16**(12):1836-42.
32. Alyautdin RN, et al. Delivery of loperamide across the blood–brain barrier with polysorbate 80-coated polybutylcyanoacrylate nanoparticles. *Pharm Res* 1997;**14**(3):325-8.
33. Alyautdin RN, et al. Significant entry of tubocurarine into the brain of rats by adsorption to polysorbate 80-coated polybutylcyanoacrylate nanoparticles: an in situ brain perfusion study. *J Microencapsul* 1998;**15**(1):67-74.
34. Kreuter J. Nanoparticulate systems for brain delivery of drugs. *Adv Drug Deliv Rev* 2001;**47**(1):65-81.
35. Kreuter J. Influence of the surface properties on nanoparticle-mediated transport of drugs to the brain. *J Nanosci Nanotechnol* 2004;**4**(5):484-8.
36. Fernandes E, et al. New trends in guided nanotherapies for digestive cancers: a systematic review. *J Control Release* 2015;**209**:288-307.
37. Field LD, et al. Peptides for specifically targeting nanoparticles to cellular organelles: quo vadis? *Acc Chem Res* 2015;**48**(5):1380-90.
38. Wohlfart S, Gelperina S, Kreuter J. Transport of drugs across the blood–brain barrier by nanoparticles. *J Control Release* 2012;**161**(2):264-73.
39. Lajoie JM, Shusta EV. Targeting receptor-mediated transport for delivery of biologics across the blood–brain barrier. *Annu Rev Pharmacol Toxicol* 2015;**55**:613-31.
40. Kuznetsova NR, et al. Hemocompatibility of liposomes loaded with lipophilic prodrugs of methotrexate and melphalan in the lipid bilayer. *J Control Release* 2012;**160**(2):394-400.
41. Singh S, et al. Mild oxidation of thiofunctional polymers to cytocompatible and stimuli-sensitive hydrogels and nanogels. *Macromol Biosci* 2013;**13**(4):470-82.
42. Groll J, et al. Biocompatible and degradable nanogels via oxidation reactions of synthetic thiomers in inverse miniemulsion. *J Polym Sci A Polym Chem* 2009;**47**(20):5543-9.
43. Bode GH, et al. Detection of peptide-based nanoparticles in blood plasma by ELISA. *PLoS One* 2015;**10**(5)e0126136.
44. Weksler BB, et al. Blood–brain barrier-specific properties of a human adult brain endothelial cell line. *FASEB J* 2005;**19**(13):1872-4.
45. Demeule M, et al. Identification and design of peptides as a new drug delivery system for the brain. *J Pharmacol Exp Ther* 2008;**324**(3):1064-72.
46. Fazakerley JK. Pathogenesis of Semliki Forest virus encephalitis. *J Neurovirol* 2002;**8**(Suppl 2):66-74.
47. De Jong WH, Borm PJ. Drug delivery and nanoparticles:applications and hazards. *Int J Nanomedicine* 2008;**3**(2):133-49.
48. Araujo F, et al. Safety and toxicity concerns of orally delivered nanoparticles as drug carriers. *Expert Opin Drug Metab Toxicol* 2014:1-13.
49. Kasper J, et al. Interactions of silica nanoparticles with lung epithelial cells and the association to flotillins. *Arch Toxicol* 2013;**87**(6):1053-65.
50. Freese C, et al. Uptake of poly(2-hydroxypropylmethacrylamide)-coated gold nanoparticles in microvascular endothelial cells and transport across the blood–brain barrier. *Biomater Sci* 2013;**1**(8):824-33.
51. Glebov OO, Bright NA, Nichols BJ. Flotillin-1 defines a clathrin-independent endocytic pathway in mammalian cells. *Nat Cell Biol* 2006;**8**(1):46-54.
52. Bockenhoff A, et al. Comparison of five peptide vectors for improved brain delivery of the lysosomal enzyme arylsulfatase a. *J Neurosci* 2014;**34**(9):3122-9.
53. Demeule M, et al. Conjugation of a brain-penetrant peptide with neurotensin provides antinociceptive properties. *J Clin Invest* 2014;**124**(3):1199-213.
54. Bruun J, et al. Investigation of enzyme-sensitive lipid nanoparticles for delivery of siRNA to blood–brain barrier and glioma cells. *Int J Nanomedicine* 2015;**10**:5995-6008.
55. Pernot M, et al. Stability of peptides and therapeutic success in cancer. *Expert Opin Drug Metab Toxicol* 2011;**7**(7):793-802.